Vps20p and Vta1p interact with Vps4p and function in multivesicular body sorting and endosomal transport in *Saccharomyces cerevisiae*

Sebastian C. L. Yeo[1,††], Linghui Xu[1,††], Jihui Ren[2,*,††], Victoria J. Boulton[1], Mahendra D. Wagle[1,†], Cong Liu[1,‡], Gang Ren[1,§], Peisze Wong[1], Regina Zahn[1,¶], Piriya Sasajala[1,], Hongyuan Yang[2], Robert C. Piper[3] and Alan L. Munn[1,2,4,§,‡‡]**

[1]Institute of Molecular and Cell Biology, The National University of Singapore, Singapore, 117609, Singapore
[2]Department of Biochemistry, Faculty of Medicine, The National University of Singapore, Singapore, 119260, Singapore
[3]Department of Physiology and Biophysics, University of Iowa, Iowa City, 52242, IA, USA
[4]Institute for Molecular Bioscience, University of Queensland, Brisbane, QLD, 4072, Australia

*Present address: Biosciences Program, University of Iowa, Iowa City, 52242, IA, USA
†Present address: Temasek Life Sciences Laboratory, Singapore
‡Present address: Genome Damage and Stability Centre, School of Biological Sciences, University of Sussex, UK
§Present address: Institute for Molecular Bioscience, University of Queensland, Brisbane, QLD, 4072, Australia
¶Present address: Deutsche Krebsforschungszentrum, Heidelberg, Germany
**Present address: University of Edinburgh, Edinburgh, UK
††These authors contributed equally
‡‡Author for correspondence (e-mail: a.munn@imb.uq.edu.au)

Accepted 7 July 2003
Journal of Cell Science 116, 3957-3970 © 2003 The Company of Biologists Ltd
doi:10.1242/jcs.00751

Summary

Vps4p (End13p) is an AAA-family ATPase that functions in membrane transport through endosomes, sorting of soluble vacuolar proteins to the vacuole, and multivesicular body (MVB) sorting of membrane proteins to the vacuole lumen. In a yeast two-hybrid screen with Vps4p as bait we isolated *VPS20* (*YMR077c*) and the novel open reading frame *YLR181c*, for which the name *VTA1* has recently been assigned (Saccharomyces Genome Database). Vps4p directly binds Vps20p and Vta1p in vitro and binding is not dependent on ATP – conversely, Vps4p binding to Vps20p is partially sensitive to ATP hydrolysis. Both ATP binding [Vps4p-(K179A)] and ATP hydrolysis [Vps4p-(E233Q)] mutant proteins exhibit enhanced binding to Vps20p and Vta1p in vitro. The Vps4p-Vps20p interaction involves the coiled-coil domain of each protein, whereas the Vps4p-Vta1p interaction involves the (non-coiled-coil) C-terminus of each protein. Deletion of either *VPS20* (*vps20Δ*) or *VTA1* (*vta1Δ*) leads to similar class E Vps$^-$ phenotypes resembling those of *vps4Δ*, including carboxypeptidase Y (CPY) secretion, a block in ubiquitin-dependent MVB sorting, and a delay in both post-internalisation endocytic transport and biosynthetic transport to the vacuole. The vacuole resident membrane protein Sna3p (whose MVB sorting is ubiquitin-independent) does not appear to exit the class E compartment or reach the vacuole in cells lacking Vps20p, Vta1p or Vps4p, in contrast to other proteins whose delivery to the vacuole is only delayed. We propose that Vps20p and Vta1p regulate Vps4p function in vivo.

Key words: AAA-ATPase, Endocytosis, Endosome, Lysosome, LYST/beige, Chediak-Higashi syndrome

Introduction

Endosomes coordinate endocytic and biosynthetic membrane traffic to lysosomes (Mellman, 1996). In *Saccharomyces cerevisiae*, three types of endosome have been characterised: early/recycling endosome, prevacuolar compartment (PVC), and multivesicular body (MVB)/late endosome. Early/recycling endosomes and PVCs are smaller and often cortical, whereas MVBs/late endosomes are larger, contain internal vesicles, and are often adjacent to the vacuole (yeast lysosome equivalent) (Hicke et al., 1997; Mulholland et al., 1999; Prescianotto-Baschong and Riezman, 1998; Prescianotto-Baschong and Riezman, 2002) (reviewed by Bryant and Stevens, 1998; Munn, 2000). Some vacuolar membrane proteins and internalised surface proteins are sorted into internal vesicles during transport through endosomes in a process known as MVB sorting and are ultimately delivered to the vacuole lumen. Other membrane proteins are retained on the limiting membrane of endosomes and are delivered to the vacuole limiting membrane (Piper and Luzio, 2001). Soluble vacuolar proteins are also delivered to the vacuole via the secretory pathway. They are synthesised as larger precursors, translocated into the ER lumen, and after transport to the late Golgi are sorted by the sorting receptor Vps10p into a distinct PVC-directed class of transport vesicle. In the vacuole they are processed to the mature form. Vacuolar protein sorting (*vps*) mutants secrete soluble vacuolar proteins into the medium because of defects in this sorting process (Bryant and Stevens, 1998).

One subset of *VPS* genes (class E *VPS*) is required for MVB sorting. Class E *vps* mutants accumulate newly synthesized soluble and membrane-associated vacuolar proteins and late Golgi proteins (e.g. Vps10p) in an enlarged endocytic compartment adjacent to the vacuole (known as the ‘class E compartment’) (Raymond et al., 1992; Davis et al., 1993; Piper

et al., 1995; Cereghino et al., 1995; Rieder et al., 1996; Odorizzi et al., 1998; Babst et al., 1997; Babst et al., 1998). A key player in MVB sorting, and the only class E Vps protein with known enzymatic activity, is the *VPS4* gene product (Vps4p). Vps4p is a member of the AAA (ATPase associated with a variety of cellular activities)-family of ATPases that also includes other membrane transport proteins such as NEM-sensitive fusion protein (NSF/Sec18p) (Babst et al., 1997; Finken-Eigen et al., 1997). Several other class E *VPS* genes encode small coiled-coil proteins that are cytosolic in wild-type cells but accumulate on endosomes in mutant cells lacking Vps4p ATPase activity (Babst et al., 1998; Babst et al., 2002). By analogy with NSF/Sec18p, which uses ATP hydrolysis to disassemble SNARE complexes on the surface of various membrane compartments, Vps4p may disassemble a coiled-coil class E Vps protein complex on the surface of endosomes (Babst et al., 1998).

We previously isolated a *vps4* mutant (*end13*, renamed *vps4-E13*) in a screen for mutants unable to survive loss of the 60 kDa subunit of vacuolar ATPase (Vma2p/Vat2p) and defective in fluid-phase endocytosis. In *vps4-E13* receptor-mediated internalisation is only slightly affected, but subsequent transport of internalised cargo through early and late endosomes to the vacuole is strongly delayed (Munn and Riezman, 1994; Zahn et al., 2001). We report here that the class E Vps protein Vps20p and the product of a novel open reading frame (ORF) *VTA1*/*YLR181c* interact with Vps4p. We show that binding of each protein to Vps4p is direct and does not require ATP, and identify the domains of each protein that mediate interaction. Loss of Vps20p or Vta1p leads to class E *vps* phenotypes similar to those caused by loss of Vps4p. We also show that whereas transport of other membrane proteins through the class E compartment to the vacuole is only delayed, the vacuole resident protein Sna3p cannot exit the class E compartment in cells lacking Vps20p, Vta1p or Vps4p.

Materials and Methods

Media, reagents, strains and plasmids

Yeast strains and plasmids used in this study are listed in Tables 1 and 2. *Escherichia coli* strain BL21 CodonPlus™ (DE3) was from Stratagene (La Jolla, CA, USA). YPUAD contained 1% yeast extract (Gibco-BRL/Life Technologies, Paisley, UK), 2% peptone (Gibco), and 2% glucose and was supplemented with 40 mg adenine and 20 mg uracil per litre. SD minimal medium was as described (Dulic et al., 1991). Geneticin 418 (G418) was from Gibco and was used at 200 μg/ml. All solid growth media contained 2% Bactoagar (Difco, Detroit, MI, USA). FM4-64 and Lucifer Yellow carbohydrazide (LY) were from Molecular Probes (Eugene, OR, USA). NBD-PC (C6) was from Avanti Polar Lipids (Alabaster, AL, USA). [^{35}S]α-factor was purified as described (Munn and Riezman, 1994). Zymolyase 20T for preparing DNA from yeast was from US Biologicals (Swampscott, MA, USA). Monoclonal anti-CPY antibody and rabbit polyclonal anti-GFP antiserum were from Molecular Probes. The horseradish peroxidase-conjugated goat anti-mouse IgG and goat anti-rabbit IgG, apyrase and protease inhibitors were from Sigma-Aldrich (St. Louis, MO, USA). Protein A Sepharose CL-4B was from Amersham/Pharmacia Biotech (Uppsala, Sweden). Immobilon-P^{SQ} membranes were from Millipore (Bedford, MA, USA). The Matchmaker LexA two-hybrid kit was from Clontech Laboratories (Palo Alto, CA, USA). Glutathione-agarose and the β-galactosidase assay kit were from Pierce (Rockford, IL, USA). Anti-pentaHIS monoclonal antibody (mouse) and NTA-Ni^{2+}-agarose were from Qiagen (Hilden, Germany).

Genetic techniques

Genetic crosses and tetrad analysis were performed as described in Adams et al. (Adams et al., 1997). Transformation of yeast with plasmid DNA was either by a modification of the lithium acetate protocol (Munn et al., 1995) or using the lithium acetate protocol recommended by Clontech for strain EGY48. Genomic DNA was prepared from *S. cerevisiae* essentially as described by Adams et al. (Adams et al., 1997) and PCR amplification was performed with *Pfu* polymerase (Stratagene) or *Taq* polymerase (Stratagene). Plasmid DNA was isolated from *S. cerevisiae* using the method of Adams et al. (Adams et al., 1997) and introduced into *E. coli* by electroporation (Dower et al., 1988). The *BAR1* gene was disrupted using a *bar1::LYS2* construct (pEK3) as described previously (Kübler and Riezman, 1993).

For functional studies, a congenic set of wild-type, *vps20Δ* and *vta1Δ* strains were analysed. Wild-type and *vps20* cells were described previously in the parental strains SF838-9D (Raymond et al., 1992). The *vps20* mutant strain was originally isolated as the *vpl10-7* mutant (*vps20-7*). The *vps20-7* strain was complemented by a low copy plasmid carrying the wild-type *VPS20* gene, but not the *vps20* gene isolated from the *vps20-7* strain (data not shown).

Table 1. Genotypes of yeast strains used in this study

Strain	Genotype	Source
RH449	*MATα his4 leu2 ura3 lys2 bar1*	Riezman strain
RH1800	*MAT***a** *his4 leu2 ura3 bar1*	Riezman strain
RH2906	*MAT***a** *end13-Δ::URA3 his4 leu2 ura3 lys2 bar1*	Zahn et al. (2001)
Y04130	*MAT***a** *vta1-Δ::KanMx his3 leu2 ura3 met15*	EUROSCARF
Y10000	*MATα his3 leu2 ura3 lys2*	EUROSCARF
AMY149	*MAT***a** *vta1-Δ:: KanMx his3 leu2 ura3 lys2*	This study
AMY158	*MAT***a** *his3 leu2 ura3 lys2*	This study
AMY162	*MAT***a** *vta1-Δ:: KanMx bar1-Δ::LYS2 his3 leu2 ura3 lys2*	This study
AMY165	*MAT***a** *bar1-Δ::LYS2 his3 leu2 ura3 lys2*	This study
AMY174	*MAT***a** *vps20-Δ::KanMx his4 leu2 ura3 bar1*	This study
EGY48	*MATα his3 trp1 ura3 LexAop(x6)-LEU2*	Clontech
SF838-9D	*MATα ade6 his4 leu2 ura3 pep4*	Raymond et al. (1992)
SF838-9D *vpl1*	*MATα vpl1(vps1)-Δ2::LEU2 ade6 his4 leu2 ura3 pep4*	Raymond et al. (1992)
SF838-9D *vpl2*	*MATα vpl2 (vps2)-7 ade6 his4 leu2 ura3 pep4*	Raymond et al. (1992)
SF838-9D *vpl10*	*MATα vpl10 (vps20)-7 ade6 his4 leu2 ura3 pep4*	Raymond et al. (1992)
SF838-9D *vpl14*	*MATα vpl14 (vps22)-6 ade6 his4 leu2 ura3 pep4*	Raymond et al. (1992)
SF838-9D *vpl12*	*MATα vpl12 (vps25)-1 ade6 his4 leu2 ura3 pep4*	Raymond et al. (1992)
SF838-9D *vpl16*	*MATα vpl16 (vps37)-2 ade6 his4 leu2 ura3 pep4*	Raymond et al. (1992)
SF838-9D *vta1Δ* (PLY3046)	*MATα vta1-Δ::KanMx ade6 his4 leu2 ura3 pep4*	This study

Table 2. Plasmids used in this study

Plasmid	Description	Source
pAM214	YCplac33 with *VPS20*	This study
pAM272	YCplac111 with *VTA1*	This study
pAM333	pLexA with full-length *VPS4* (encoding Vps4p$_{1-437/end}$)	This study
pAM349	Original library clone of *VPS20* in pB42AD (encoding Vps20p$_{3-221/end}$)	This study
pAM352	YCplac111 with full-length *VPS4* fused in-frame with yEGFP	This study
pAM377	pGEX5X-1 with full-length *VPS20* (encoding GST-Vps20p)	This study
pAM378	pGEX5X-1 with full-length *VTA1* (encoding GST-Vta1p)	This study
pAM397	YCplac111 with full-length *SNA3* fused in-frame with yEGFP	This study
pAM398	Original library clone of *VTA1* in pB42AD (encoding Vta1p$_{108-330/end}$)	This study
pAM399	pFA6a-KanMx6 with *VPS20* 5′ and 3′ flanking sequences introduced either side of KanMx6 (for disruption of *VPS20* with KanMx6)	This study
pEK3	Construct for disruption of *BAR1* with *LYS2*	Kübler and Riezman (1991)
pFA6a-KanMx6	KanMx6 cloning vector	Longtine et al. (1998)
YCplac33	*CEN4 ARS1 URA3 E. coli*/yeast shuttle vector	Gietz and Sugino (1988)
YCplac111	*CEN4 ARS1 LEU2 E. coli*/yeast shuttle vector	Gietz and Sugino (1988)
pGEX5X-1	GST fusion vector	Amersham/ Pharmacia Biotech AB
pPL967	*STE3-GFP* in *LEU2 CEN* plasmid	Urbanowski and Piper (2001)
pPL1640	*FTH1-GFP-Ub* in *URA3 CEN* plasmid	Urbanowski and Piper (2001)
pTS18	*PEP4* in *URA3 CEN* plasmid	Rothman et al. (1986)
p8op-lacZ	Two-hybrid reporter plasmid	Clontech
pLexA	Two-hybrid bait vector	Clontech
pB42AD	Two-hybrid prey vector	Clontech
pAM452	pLexA with *VPS4* fragment encoding N-terminal coiled-coil domain (encoding Vps4p$_{1-128}$)	This study
pAM453	pLexA with *VPS4* fragment encoding AAA-ATPase domain (encoding Vps4p$_{129-350}$)	This study
pAM454	pLexA with *VPS4* fragment encoding C-terminal acidic domain (encoding Vps4p$_{351-437/end}$)	This study
pAM485	pB42AD with *VPS20* fragment encoding N-terminal domain (encoding Vps20p$_{1-41}$)	This study
pAM461	pB42AD with *VPS20* fragment encoding central coiled-coil domain (encoding Vps20p$_{42-173}$)	This study
pAM486	pB42AD with *VPS20* fragment encoding C-terminal domain (encoding Vps20p$_{174-221/end}$)	This study
pAM480	pB42AD with *VPS20* fragment encoding N-terminal and coiled-coil domains (encoding Vps20p$_{1-173}$)	This study
pAM481	pB42AD with *VPS20* fragment encoding coiled-coil and C-terminal domains (encoding Vps20p$_{42-221/end}$)	This study
pAM403	pB42AD with *VTA1* fragment encoding 1st coiled-coil domain (encoding Vta1p$_{1-108}$)	This study
pAM405	pB42AD with *VTA1* fragment encoding Vta1p central domain (encoding Vta1p$_{109-231}$)	This study
pAM407	pB42AD with *VTA1* fragment encoding Vta1p 2nd coiled-coil domain (encoding Vta1p$_{232-264}$)	This study
pAM410	pB42AD with *VTA1* fragment encoding Vta1p C-terminal domain (encoding Vta1p$_{265-330/end}$)	This study
pAM482	pET11a *E. coli* T7 expression vector with *VPS4* including C-terminal 6HIS tag	This study
pAM483	pET11a *E. coli* T7 expression vector with *vps4-E233Q* including C-terminal 6HIS tag	This study
pAM484	pET11a *E. coli* T7 expression vector with *vps4-K179A* including C-terminal 6HIS tag	This study

Sequencing of the *VPS20* ORF (*YMR077c*) from the *vps20-7* strain revealed a deletion of the first nucleotide (G) in codon 20 (GTA to TA), causing the protein product to be translated out of frame (data not shown). This confirms that *YMR077c* is the ORF corresponding to *VPS20*, consistent with previous reports (Kranz et al., 2001; Howard et al., 2001; Forsberg et al., 2001). Thus, for simplicity, we refer to the *vps20-7* strain as *vps20Δ*. Y04130 (*vta1Δ::KanMx*) and the isogenic wild-type strain Y10000 were obtained from Euroscarf (European Saccharomyces Cerevisiae ARchives for Functional Analysis, Frankfurt, Germany). To introduce *vta1Δ* into the SF838-9D strain background, a PCR fragment encoding the KanMx ORF flanked by 400 bp either side of the *YLR181c* coding sequence was amplified from Y04130 genomic DNA and used to transform SF838-9D cells. G418-resistant colonies were verified for loss of *YLR181c* by PCR analysis of genomic DNA, and one isolate was retained for phenotypic analysis (PLY3046).

For α-factor assays we prepared *vps20Δ* and *vta1Δ MAT***a** strains that lack Bar, a secreted protease responsible for degradation of α-factor (*bar1*). DNA fragments corresponding to 301 to 1 nucleotide upstream and 5 to 230 nucleotides downstream of the *VPS20* coding sequence were amplified by PCR and subcloned into pFA6a-KanMx6 either side of the *KanMx* gene (Longtine et al., 1998) to create pAM399. pAM399 was digested with *Kpn*I and *Pst*I to release a fragment containing the *KanMx* cassette with *VPS20* flanking sequences and used to disrupt the *VPS20* gene in the wild-type *MAT***a** *bar1* strain RH1800. G418-resistant transformants were selected on YPUAD/G418 medium and the presence of the disruption was confirmed by PCR analysis of genomic DNA (data not shown). One *vps20Δ* haploid (AMY174) was retained for further analysis. Complementation analysis was performed with several *vps* mutant strains including the *vps2-7* (*vpl2-7*), *vps20-7* (*vpl10-7*), *vps22-6* (*vpl14-6*), *vps25-1* (*vpl12-1*) and *vps37-2* (*vpl16-2*) mutants defined in previous studies (Raymond et al., 1992) (Table 1). These studies showed that only *vps20-7* failed to complement *vps20Δ* (AMY174). Introduction of a low copy *VPS20* plasmid corrected the CPY secretion defect in AMY174.

To make congenic *vta1Δ* and wild-type strains suitable for α-factor assays, Y04130 was crossed with Y10000 and the resulting diploid subjected to tetrad dissection. Two haploids from this cross were AMY149 (*MAT***a** *lys2 vta1Δ*) and AMY158 (*MAT***a** *lys2 VTA1*). The *BAR1* gene was deleted in AMY149 and AMY158, yielding AMY162 and AMY165, respectively, which were then used for α-factor assays. The CPY missorting defect in AMY162 was complemented by the introduction of a low copy *VTA1* plasmid.

Yeast two-hybrid analysis

A bait construct expressing full-length Vps4p as a fusion to the DNA-binding domain of LexA, pLexA-Vps4 (pAM333), was constructed and introduced into yeast strain EGY48 containing the reporter plasmid p8op-LacZ (Clontech). Transformation of this strain with the pB42AD transcription activation domain vector alone did not confer significant expression of the two-hybrid reporter genes *LEU2* or *lacZ* (data not shown). An *S. cerevisiae* two-hybrid library containing genomic DNA inserts in vector pB42AD (pJG4-5) (Gyuris et al., 1993) (a gift from U. Surana, IMCB, Singapore) was transformed into this strain and colonies exhibiting expression of the *LEU2* interaction reporter gene were selected on synthetic galactose/raffinose (SG)

complete medium-Leu. The equivalent of 5×10^4-1×10^5 colonies were screened (as assessed by plating one sample of the transformed cells on SD complete medium selecting only for pLexA-Vps4 and the pB42AD library plasmids). Positive colonies were subsequently tested for blue colouration on SG complete medium containing X-gal. The library plasmid was isolated from positive colonies and retransformed into EGY48 containing p8op-LacZ and either pLexA-Vps4 or pLexA vector alone. Library plasmids that were reproducibly able to confer growth on SG complete-Leu and blue colouration on SG complete + X-gal upon retransformation into EGY48/p8op-LacZ cells containing pLexA-Vps4, but not when introduced into EGY48/p8op-LacZ cells containing pLexA vector only, were retained for further analysis. β-galactosidase activity was assayed using a kit as recommended by the manufacturer.

To identify the domains within Vps20p and Vta1p that mediate two-hybrid interaction with Vps4p, we constructed a series of plasmids expressing different fragments of Vps20p or Vta1p fused in-frame with B42AD (in pB42AD) (Table 2). To identify the domains within Vps4p that mediate two-hybrid interaction with Vps20p and Vta1p, we constructed a series of plasmids expressing different fragments of Vps4p fused in-frame with LexA (in pLexA) (Table 2). We then tested interaction of both the longer fragments of Vps20p and Vta1p encoded by the original library clones (pAM349 and pAM398, respectively) and the shorter fragments encoded by the pB42AD-based plasmids described above with full-length Vps4p (pAM333) in EGY48 carrying p8op-LacZ. We also tested interaction of full-length Vps4p (pAM333) and the shorter fragments encoded by the pLexA-based plasmids described above with the original library clones of Vps20p and Vta1p (pAM349 and pAM398, respectively) in EGY48 carrying p8op-LacZ. The strength of interaction was assessed by blue colouration on SG complete medium containing X-gal.

Construction of *VPS20* and *VTA1* complementing plasmids

The wild-type *VPS20* and *VTA1* full-length genes were amplified by PCR using *Pfu* polymerase from RH1800 yeast genomic DNA. An amount (400 bp) of upstream sequence was included for *VPS20* and 1kb for *VTA1*. These fragments were cloned into the low-copy plasmids YCplac33 and YCplac111, respectively (Gietz and Sugino, 1988). The inserts of YCp-*VPS20* (pAM214) and YCp-*VTA1* (pAM272) were confirmed by sequencing. YCp-*VPS20* and YCp-*VTA1* were able to fully complement the Vps$^-$ defect of *vps20Δ* and *vta1Δ*, respectively.

In vitro binding assays

To test whether Vps20p and Vta1p can bind Vps4p in vitro we expressed Vps20p and Vta1p as fusions to glutathione S-transferase (GST). The full-length *VPS20* and *VTA1* coding sequences were amplified by PCR from pAM214 and pAM272 and cloned into pGEX5X-1 (Amersham/Pharmacia Biotech) in-frame and 3′ of GST. *vps4E233Q-6HIS* and *vps4K179A-6HIS* were constructed by amplifying *VPS4* by PCR from yeast genomic DNA using internal mutagenic primers and 5′ and 3′ *VPS4* flanking primers including *Nde*I and *Bam*HI sites, respectively. Wild-type *VPS4-6HIS* was constructed by amplifying *VPS4* using the flanking primers only. The 3′ flanking primers also encoded six histidine residues fused in-frame with the Vps4p C-terminus. Wild-type *VPS4-6HIS*, *vps4E233Q-6HIS* and *vps4K179A-6HIS* were cloned into pET11a between the *Nde*I and *Bam*HI sites and 3′ of the T7 promoter. Inserts and frame were confirmed by sequencing. The GST- and 6HIS-tagged proteins were expressed in BL21-CodonPlus^{TM} (DE3) *E. coli* and purified using glutathione-agarose or Ni^{2+}-NTA agarose beads, respectively. The *VPS4* gene was amplified without the terminator codon from RH1800 genomic DNA and ligated into a YCplac111-based plasmid encoding yEGFP (a gift of B. Winsor, IBMC, University of Strasbourg, France) to create a fusion in which the C-terminus of *VPS4* is fused to yEGFP (pAM352). pAM352 fully complemented the Vps$^-$ phenotype of *vps4Δ* and therefore encodes a functional fusion protein (data not shown).

The binding of Vps4p in yeast lysates to recombinant Vps20p and Vta1p was assayed as follows. *vps4Δ* (RH2906) cells expressing Vps4p-GFP (pAM352) or Vps4p with no tag (pEND13.1) (Zahn et al., 2001) were grown in SD minimal medium and subjected to glass bead lysis in extraction buffer (20 mM HEPES, 200 mM sorbitol, 100 mM potassium acetate, 1 mM EDTA, pH7.5) containing protease inhibitors (10 μg/ml aprotinin, 5 μg/ml leupeptin, 8 μg/ml pepstatin, 1 mM phenylmethylsulphonylfluoride) and 1 mM DTT. Low-speed centrifugation (700 ***g***) was used to remove unbroken cells and the resulting supernatant (S1) was fractionated by differential centrifugation into 16,000 ***g*** and 100,000 ***g*** pellets (P2, P3) and a 100,000 ***g*** supernatant (S3). The S3 fraction was supplemented with 20 mM $MgCl_2$ and divided in two. One sample was incubated with apyrase (5.7 U/ml final) for 10 minutes at room temperature to deplete endogenous ATP, whereas the other was incubated without apyrase. The apyrase activity under these buffer and temperature conditions was approximately 25% of that specified by the manufacturer (i.e. 1.4 U/ml final) (data not shown). Both ATP-depleted and untreated lysates were then incubated with beads bearing GST-Vps20p, GST-Vta1p or GST only at 4°C for 12 hours. Unbound protein was precipitated with trichloroacetic acid, dissolved in Laemmli sample buffer, and neutralised with 1 M Tris base. The beads were washed with extraction buffer prior to elution of the bound proteins by heating in Laemmli sample buffer. Proteins in each sample were resolved by SDS-PAGE, transferred to Immobilon-P^{SQ} PVDF membranes and Vps4p-GFP was detected with an anti-GFP antiserum and enhanced chemiluminescence.

To test direct binding of Vps4p to Vps20p and Vta1p, 6HIS-tagged wild-type or mutant Vps4p were expressed in and purified from *E. coli* as described above. Vps4p-6HIS was eluted from the beads with 250 mM imidazole in PBS containing 1mM β-mercaptoethanol and 0.05% Tween 20 and dialysed against extraction buffer containing 1 mM DTT. For binding assays, 5-10 μg of purified wild-type or mutant Vps4-6HIS in extraction buffer containing 1 mM DTT and 1 mM phenylmethylsulphonylfluoride were used. Each sample was supplemented to 20 mM $MgCl_2$ and 0.1% Triton X-100 and incubated with beads bearing GST-Vps20p (500 μg), GST-Vta1p (100 μg) or GST (500 μg) in the presence or absence of 1 mM ATP at 4°C for 12 hours. The samples were processed as above (with the slight modification that unbound samples were supplemented with bovine serum albumin as carrier prior to precipitation with trichloroacetic acid). After SDS-PAGE Vps4p-6HIS was detected by immunoblotting using a pentaHIS-specific monoclonal antibody and enhanced chemiluminescence.

Endocytosis assays

Fluid-phase endocytosis was measured by vacuolar accumulation of the membrane-impermeant fluorescent dye LY carbohydrazide following incubation for 1 hour at 24°C as described in Munn et al. (Munn et al., 1999). Endocytosis of plasma membrane was assayed using the lipid-soluble styryl dye FM4-64 (Vida and Emr, 1995). Cells were incubated with 2 μM FM4-64 at 0°C for 30 minutes to label the cell surface. Then the cells were washed on ice, resuspended in fresh medium at 30°C (0’), and transport of the dye from the cell surface to the vacuole was assessed at various time points. [^{35}S]α-factor internalisation assays were performed at 30°C using the continuous presence protocol (Dulic et al., 1991). [^{35}S]α-factor degradation assays were performed at 30°C using the pulse-chase protocol (Dulic et al., 1991).

Carboxypeptidase Y missorting test

To assess maturation of newly synthesised CPY and processing of the receptor for soluble vacuolar proteins (Vps10p) we

immunoprecipitated CPY and Vps10p from cells labeled with [^{35}S]Methionine/cysteine as described (Piper et al., 1995). For this analysis, strains were converted to Pep$^+$ by transformation with pTS18 (*PEP4* centromeric plasmid).

Multivesicular body sorting assay

Localisation of Ste3-GFP, Fth1-GFP-Ub, Sna3-GFP and NBD-PC were performed as previously described (Bilodeau et al., 2002). The Sna3-GFP reporter used here was made by amplifying *SNA3* without a termination codon by PCR using RH1800 genomic DNA and then subcloning it into a YCplac111-based plasmid 5′ and in-frame with yEGFP (pAM397). This places the GFP at the Sna3p C-terminus.

Fluorescence microscopy

All microscopy was performed using an Olympus BX-60 microscope fitted with Differential Interference Contrast (DIC) light filters and appropriate fluorescence light filters.

Results

Vps20p and Vta1p interact with Vps4p

A bait plasmid encoding full-length Vps4p fused to the LexA DNA binding domain (LexA), pLexA-Vps4 (pAM333), was used to screen a library of *Saccharomyces cerevisiae* genomic DNA fragments fused to the B42 transcription activation domain (B42AD) to identify novel Vps4p two-hybrid interactors. Of 20 library plasmids that activated the reporters upon isolation and retransformation into the EGY48 tester strain containing pLexA-Vps4, four contained identical inserts from ORF *YMR077c*/*VPS20*/*CHM6* (encoding residues 3-221 of 221) and six contained identical inserts from the novel ORF *YLR181c* (for which the name *VTA1* has recently been assigned by L. Eguez and S. Garrett, Saccharomyces Genome Database) (encoding residues 108-330 of 330) fused in-frame with B42AD (Fig. 1A). One *VPS20* clone (pAM349) and one *VTA1* clone (pAM398) were retained for further analysis. Both pAM349 and pAM398 conferred strong activation of the reporters in the presence of pLexA-Vps4 after 2 days of incubation that did not increase further after 4 days (Fig. 1B). However, the pLexA-Vps4 bait and pB42AD-based library plasmids did not activate the reporters either alone or in combination with the empty pB42AD or pLexA vectors, respectively, even after 4 days of incubation (Fig. 1B). Quantification of reporter expression by β-galactosidase activity assays confirmed the results of the plate assays (Fig. 1C).

We next used the yeast two-hybrid system to map the domains of Vps4p, Vps20p and Vta1p that mediate the interactions. Two-hybrid plasmids expressing various fragments of Vps4p, Vps20p and Vta1p were constructed (Fig. 1A, Table 2). The results of two-hybrid analyses using these constructs as well as pLexA-Vps4 (pAM333) and the original Vps20p and Vta1p library clones (pAM349 and pAM398, respectively) are shown in Tables 3 and 4. The N-terminal coiled-coil domain of Vps4p interacted very strongly with Vps20p, but not with Vta1p, whereas the C-terminal acidic domain of Vps4p interacted with both proteins, but more strongly with Vta1p. The AAA-ATPase domain did not interact with either Vps20p or Vta1p. A fragment containing the central coiled-coil domain plus the C-terminal domain of Vps20p was necessary and sufficient for interaction with full-length Vps4p. In the case of Vta1p, the C-terminal domain was sufficient for interaction with Vps4p.

Vps20p and Vta1p directly bind Vps4p in vitro

We next tested whether Vps20p or Vta1p bind Vps4p in vitro. Vps20p and Vta1p were expressed as GST fusions in bacteria and purified. Beads bearing GST-Vps20p or GST-Vta1p, but not beads bearing GST alone, precipitated GFP-tagged Vps4p from yeast lysates (Fig. 2). We also tested the ability of Vps4p-GFP to associate with GST-Vps20p and GST-Vta1p after depletion of ATP from the lysates. The association of Vps4p-GFP with GST-Vps20p, but not GST-Vta1p, was slightly enhanced (approximately twofold) by ATP depletion (Fig. 2). Strong association of Vps4p-GFP with both GST-Vps20p and GST-Vta1p was also observed after depletion of free Mg^{2+} (data not shown). Hence, the in vitro association of Vps4p with Vps20p and Vta1p does not require ATP, and in the case of Vps20p it is slightly sensitive to ATP hydrolysis. Similar results were obtained using a Vps4p construct with a C-terminal myc-epitope (data not shown).

In order to test whether Vps4p directly binds Vps20p and Vta1p in vitro and to further examine the role of ATP binding, we expressed wild-type Vps4p-6HIS, Vps4pE233Q-6HIS (ATP hydrolysis defective) and Vps4pK179A-6HIS (ATP binding defective) in bacteria. Each protein was affinity purified and used in pulldown assays using beads bearing GST-Vps20p, GST-Vta1p or GST only (Fig. 3). Wild-type Vps4p-6HIS bound both GST-Vps20p and GST-Vta1p, but not GST alone, in vitro, indicating that the association of Vps4p with Vps20p and Vta1p is direct and not mediated by other proteins. Binding was observed in the presence and in the absence of added ATP, in agreement with the results described above for Vps4p-GFP in yeast lysates. Binding of Vps4p-6HIS to GST-Vta1p was not affected by addition of ATP, but binding to GST-Vps20p was stronger when ATP was omitted. These findings are in agreement with the results described above that association of Vps4p-GFP in yeast lysates with GST-Vps20p is stronger after depleting the lysate of ATP. Vps4pE233Q-6HIS and Vps4pK179A-6HIS also bound to both GST-Vps20p and GST-Vta1p, but not to GST alone, indicating in another way that ATP binding is not necessary for association of Vps4p with Vps20p or Vta1p. In the case of both mutant Vps4p-6HIS proteins, binding to GST-Vps20p and GST-Vta1p was significantly enhanced compared with wild-type Vps4p-6HIS. As expected, binding of the mutant Vps4p-6HIS proteins to GST-Vps20p and GST-Vta1p was not significantly affected by addition of ATP.

Vps20p and Vta1p are required for efficient post-internalisation transport of α-factor

We next determined whether Vps20p or Vta1p are required for receptor-mediated endocytosis. Receptor-mediated uptake of [^{35}S]α-factor was assayed at 30°C in *vps20Δ* and *vta1Δ* and the corresponding wild-type strains (Fig. 4). [^{35}S]α-factor was internalised by all four strains, although *vps20Δ* and *vta1Δ* showed slightly slower kinetics and this difference was reproducible. To investigate whether post-internalisation

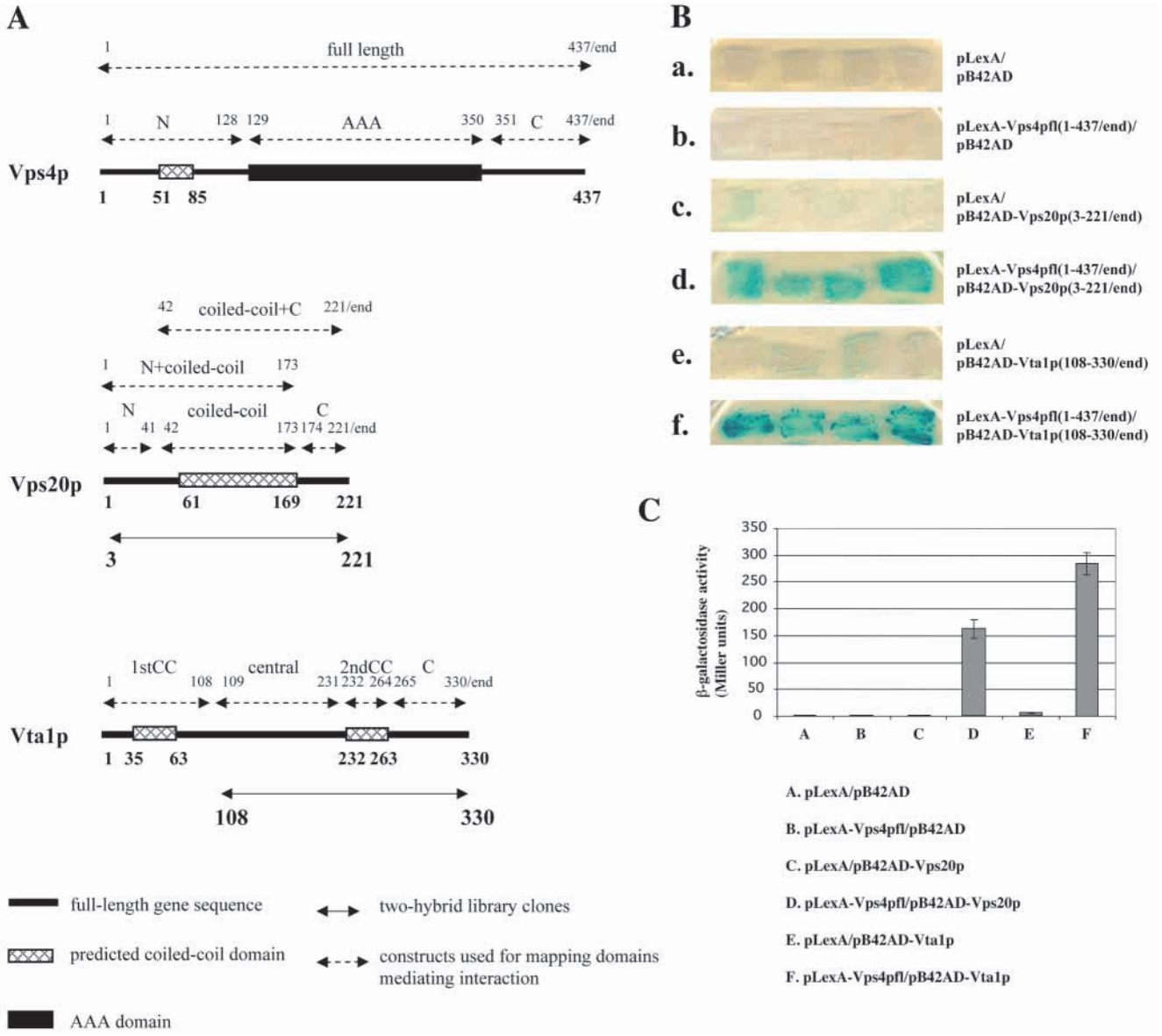

Fig. 1. Vps4p interacts with Vps20p and Vta1p. (A) A schematic showing the predicted domain structure of Vps20p, Vta1p and Vps4p, the fragments of Vps20p and Vta1p encoded by the two-hybrid library plasmids pB42AD-*VPS20* (pAM349) and pB42AD-*VTA1* (pAM398), and the various constructs used to map the domains that interact. Cross-hashed boxes represent domains predicted to have a high propensity (≥0.5) to form coiled-coil structure as assessed using the COILS algorithm (Lupas et al., 1991). Numbers refer to amino acid residues. Library plasmids are depicted using solid lines and constructs used for mapping using broken lines. (B) Yeast two-hybrid interactions of Vps4p with Vps20p and Vta1p. Yeast strain EGY48 carrying the reporter plasmid p8op-LacZ together with either pLexA vector alone or pLexA-*VPS4* (pAM333), and either pB42AD vector alone, pB42AD-*VPS20* or pB42AD-*VTA1* were plated on SD complete medium lacking uracil, histidine and tryptophan to select for the p8op-LacZ, pLexA-based and pB42AD-based plasmids, respectively. After the strains had grown sufficiently they were replica plated to synthetic galactose/raffinose (SG) complete medium containing X-gal to test expression of the *lacZ* two-hybrid interaction reporter gene. The plates were photographed after 4 days at 30°C. Shown are patches representing four independent transformants for each plasmid combination (a-f). (C) Quantification of yeast two-hybrid interactions. Each of the strains in B was assayed for β-galactosidase activity as a measure of the strength of two-hybrid interaction. Activities (in Miller units) represent the means obtained from assaying three independent transformants. Error bars, +/–s.e.m.

transport of [^{35}S]α-factor to the vacuole is affected in the mutants, we assayed the kinetics of [^{35}S]α-factor degradation at 30°C. Both the *vps20Δ* and *vta1Δ* mutations significantly delayed the vacuolar delivery and consequent degradation of the internalised [^{35}S]α-factor (as assessed by loss of intact [^{35}S]α-factor spots and appearance of degraded [^{35}S]α-factor spots) (Fig. 5).

Loss of Vps20p or Vta1p result in CPY secretion and accumulation of Ste3-GFP in an endosomal compartment

To characterize the role of Vps20p and Vta1p in vacuolar protein sorting and MVB sorting, we constructed congenic *vps20Δ* and *vta1Δ* mutant strains using the SF838-9D *MAT*α parental strain. SF838-9D has been extensively used for

Table 3. Two-hybrid interactions between Vps20p and Vta1p and different domains of Vps4p

	pLexA	pLexA-Vps4pfl (1-437/end)	pLexA-Vps4p-N (1-128)	pLexA-Vps4p-AAA (129-350)	pLexA-Vps4p-C (351-437/end)
pB42AD	–	–	–	–	–
pB42AD-Vps20p (3-221/end)	–	+	++	–	+

	pLexA	pLexA-Vps4p (1-437/end)	pLexA-Vps4p-N (1-128)	pLexA-Vps4p-AAA (129-350)	pLexA-Vps4p-C (351-437/end)
pB42AD	–	–	–	–	–
pB42AD-Vtalp (108-330/end)	–	++	–	–	+

–, no interaction; +, interaction; ++, very strong interaction.

Table 4. Two-hybrid interactions between Vps4p and different domains of Vps20p and Vta1p

	pB42AD	pB42AD-Vps20p (3-221/end)	pB42AD-Vps20p-N (1-41)	pB42AD-Vps20p-longCC (42-173)	pB42AD-Vps20p-C (174-221/end)	pB42AD-Vps20p-N+longCC (1-173)	pB42AD-Vps20p-longCC+C (42-221/end)
pLexA	–	–	–	–	–	–	–
pLexA- Vps4pfl (1-437/end)	–	+	–	–	–	–	++

	pB42AD	pB42AD-Vtalp (108-330/end)	pB42AD-Vtalp-1st CC (1-108)	pB42AD-Vtalp-central (109-231)	pB42AD-Vtalp-2nd CC (232-264)	pB42AD-Vtalp-C (265-330/end)
pLexA	–	–	–	–	–	–
pLexA-Vps4pfl (1-437/end)	–	++	–	–	–	++

–, no interaction; +, interaction; ++, very strong interaction.

analysis of these processes (Raymond et al., 1992) and carries the *pep4-3* mutation that allows lumenal vesicles to accumulate in the vacuole.

Ste3p is the plasma membrane receptor for the secreted yeast mating pheromone **a**-factor. In wild-type cells, Ste3-GFP travels to the cell surface and is then rapidly endocytosed and delivered to the vacuole. The Ste3-GFP protein typically accumulates to high levels in the lumen of wild-type vacuoles indicative of proper MVB sorting to intralumenal vesicles (Urbanowski and Piper, 2001). To test whether Vps20p and Vta1p are required for MVB sorting of Ste3p, we localised Ste3-GFP in wild-type cells and in *vps20Δ* and *vta1Δ* cells carrying the low copy YCp-*VPS20* plasmid or YCp-*VTA1* plasmid or empty vector only (Fig. 6). In both *vps20Δ* and *vta1Δ* cells Ste3-GFP was found on the limiting membrane of the vacuole as well as in 2-3 punctate structures adjacent to the vacuole, but not in the vacuole lumen. The punctate structures adjacent to the vacuole were similar to the class E compartments observed for other class E *vps* mutants (Raymond et al., 1992). The defects in MVB sorting of Ste3-GFP were corrected when the *vps20Δ* strain or *vta1Δ* strain was transformed with the corresponding wild-type gene borne on a low-copy plasmid (Fig. 6).

To test whether Vta1p, like Vps20p, is required for efficient vacuolar protein sorting, we compared the sorting of the soluble vacuolar hydrolase carboxypeptidase Y (CPY) to the vacuole in cells lacking Vps20p or Vta1p. Both the *vps20Δ* and *vta1Δ* mutants secreted ~40% of CPY after a 60-minute chase (Fig. 7). Previous studies have shown that CPY secretion is because of depletion of the CPY receptor (Vps10p) from the Golgi and its accumulation within the class E endosomal compartment. In Pep^+ cells the class E compartment is proteolytically active and the delivery and accumulation of Vps10p in the class E compartment can be monitored by pulse/chase labeling and immunoprecipitation of Vps10p (Piper et al., 1995). In *vps20Δ* and *vta1Δ*, a significant amount of newly synthesised Vps10p undergoes a *PEP4*-dependent cleavage after a 60-minute chase consistent with what has been observed for other class E *vps* mutants (Cereghino et al., 1995).

Vps20p and Vta1p are required for MVB formation

The defects in MVB sorting of Ste3-GFP in *vps20Δ* and *vta1Δ* mutants was consistent with a role of Vps20p and Vta1p in MVB formation. This process incorporates a variety of membrane proteins into intralumenal vesicles that accumulate in the vacuoles of *pep4* mutant yeast (Piper and Luzio, 2001). For some proteins, their delivery to the vacuole interior is dependent on attachment of ubiquitin, whereas the delivery of other proteins is ubiquitin-independent (Katzmann et al., 2002). The ubiquitin-dependent MVB sorting mechanism is exemplified by the chimeric Fth1-GFP-Ub reporter protein. Fth1p is an iron transporter whose distribution is restricted to the limiting membrane of the vacuole, but the Fth1-GFP-Ub chimera is a substrate for ubiquitin-dependent MVB sorting and in wild-type cells localises to vacuolar intralumenal vesicles (Urbanowski and Piper, 2001). The ubiquitin-independent sorting mechanism is exemplified by the Sna3-GFP reporter protein. Sna3p is an integral membrane protein first identified as a component of vacuolar intralumenal

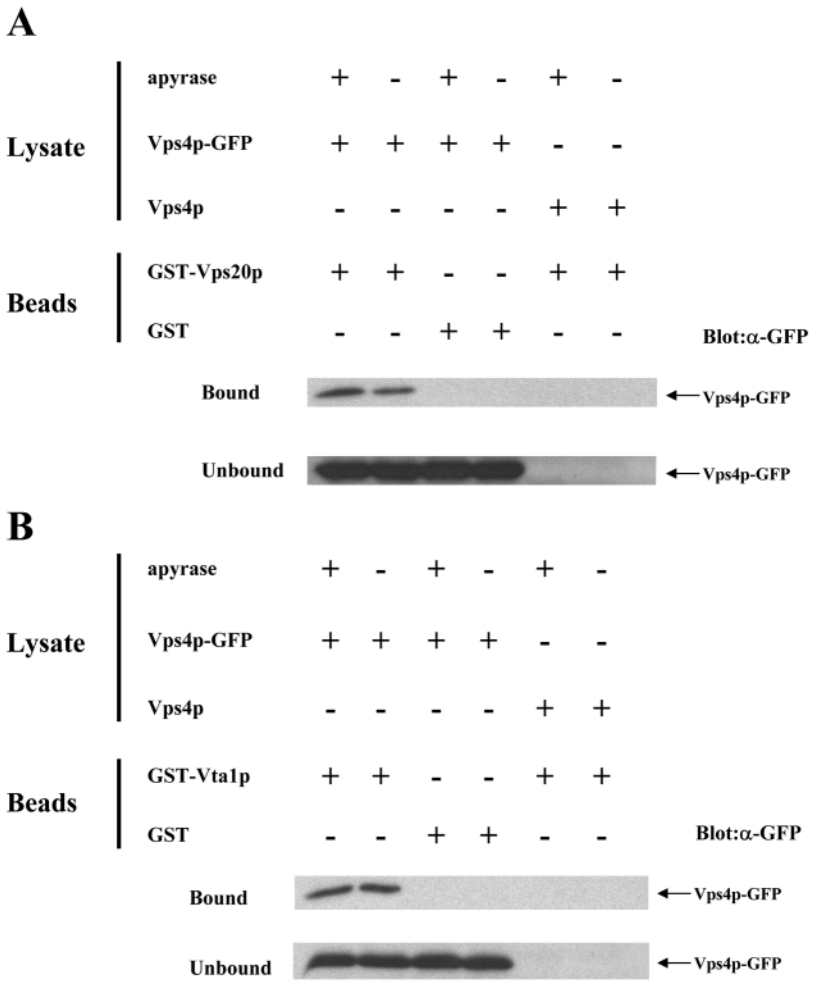

Fig. 2. Vps4p in yeast lysates associates with Vps20p and Vta1p and association is ATP-independent. Vps20p and Vta1p were expressed as GST fusions in *E. coli* and purified on glutathione-agarose beads. Vps4p, either tagged with GFP or without tag, was expressed from a centromeric plasmid in *vps4Δ* (RH2906). Lysates were prepared from both strains and a 100,000 ***g*** supernatant (S3) was supplemented with 20 mM $MgCl_2$ and incubated with beads bearing GST only or GST-Vps20p (A), or with beads bearing GST only or GST-Vta1p (B) with or without pretreatment of the lysates with apyrase to deplete endogenous ATP. Unbound proteins (unbound) were recovered in the supernatants. After washing the beads, the specifically bound proteins (bound) were eluted by heating in Laemmli sample buffer. Proteins in both bound and unbound samples were resolved by SDS-PAGE, and transferred to PVDF membranes. Vps4p-GFP was detected by immunoblotting with a GFP-specific polyclonal antiserum. In each set of experiments the exposure times for the gels containing bound and unbound samples were identical.

vesicles. MVB sorting of Sna3p is not affected by substitution of its two cytoplasmic lysines (potential ubiquitination sites) or by lowered free ubiquitin levels (e.g. in a *doa4Δ* mutant) and is thus ubiquitin-independent (Reggiori and Pelham, 2001). In wild-type cells, we found that both Fth1-GFP-Ub and Sna3-GFP were localised to the vacuole lumen (Fig. 8). However, in either *vps20Δ* or *vta1Δ* cells, Fth1-GFP-Ub accumulated on both the limiting membrane of the vacuole as well as in large 'class E' structures similar to where Ste3-GFP accumulated (Figs 6, 8). Sna3-GFP was also excluded from the vacuole interior, but far less was observed on the limiting membrane of the vacuole. Rather, Sna3-GFP was found almost exclusively within class E compartments. Morphometric analysis of fluorescence intensity between Ste3-GFP, Fth1-GFP-Ub and Sna3-GFP confirmed that the exclusive localisation of Sna3-GFP to the class E compartment was not because of the overall level of these proteins or limits in fluorescence detection.

Aside from the inability to sort membrane proteins into intralumenal vesicles, at least some class E *vps* mutants (including *vps4*) are also unable to perform lipid sorting events required to make lumenal vesicles. Previously, NBD-PC has been shown to be a lipid marker of the intralumenal vesicles (Bilodeau et al., 2002; Hanson et al., 2002). To test whether Vps20p and Vta1p are (like Vps4p) required for sorting of lipids into intralumenal vesicles, we compared the distribution of internalised NBD-PC in wild-type, *vps20Δ* and *vta1Δ* mutants (Fig. 9). In wild-type cells, NBD-PC was sorted into vesicles in the vacuole lumen. In *vps20Δ* or *vta1Δ* cells, however, NBD-PC was not sorted into intralumenal vesicles, but remained on the limiting membrane of the vacuole as well as in class E endosomal compartments. Thus sorting of lipids (as well as proteins) to form intralumenal vesicles requires both Vps20p and Vta1p.

Vps20p and Vta1p are required for efficient endocytosis of fluid-phase and membrane markers from the cell surface to the vacuole

We next tested whether Vps20p and Vta1p play a role in endocytic membrane traffic of bulk fluid to the vacuole. Wild-type, *vps20Δ* and *vta1Δ* cells were incubated in the presence of the fluid-phase endocytic marker LY and accumulation of the dye in the vacuole was examined (Fig. 8). Low levels of LY did accumulate in the vacuoles of *vps20Δ* and *vta1Δ* cells, but markedly less than in the vacuoles of wild-type cells. Therefore, both Vps20p and Vta1p are important for fluid-phase transport to the vacuole, although not essential.

We next examined whether Vps20p and Vta1p are important for bulk membrane transport from the cell surface to the vacuole. The lipid dye FM4-64 is a membrane-soluble dye that binds to the plasma membrane and is internalised by endocytosis and delivered to the vacuole membrane (Vida and Emr, 1995). Cell surface membranes of wild-type, *vps20Δ* and *vta1Δ* cells were labeled with FM4-64 at 0°C, and cells were then warmed to 30°C and assessed for distribution of FM4-64 at various times (Fig. 10). At early times after shift to 30°C, FM4-64 labeled small punctate structures and at later times it accumulated in 1-2 large late-endosomal/prevacuolar structures adjacent to the vacuole. By 30 minutes, FM4-64 could clearly be seen on the vacuole limiting membrane in wild-type cells. In contrast, the bulk of FM4-64 remained in large endosomal structures in both the *vps20Δ* and *vta1Δ* cells, indicating a delay in transport from the class E compartment to the vacuole.

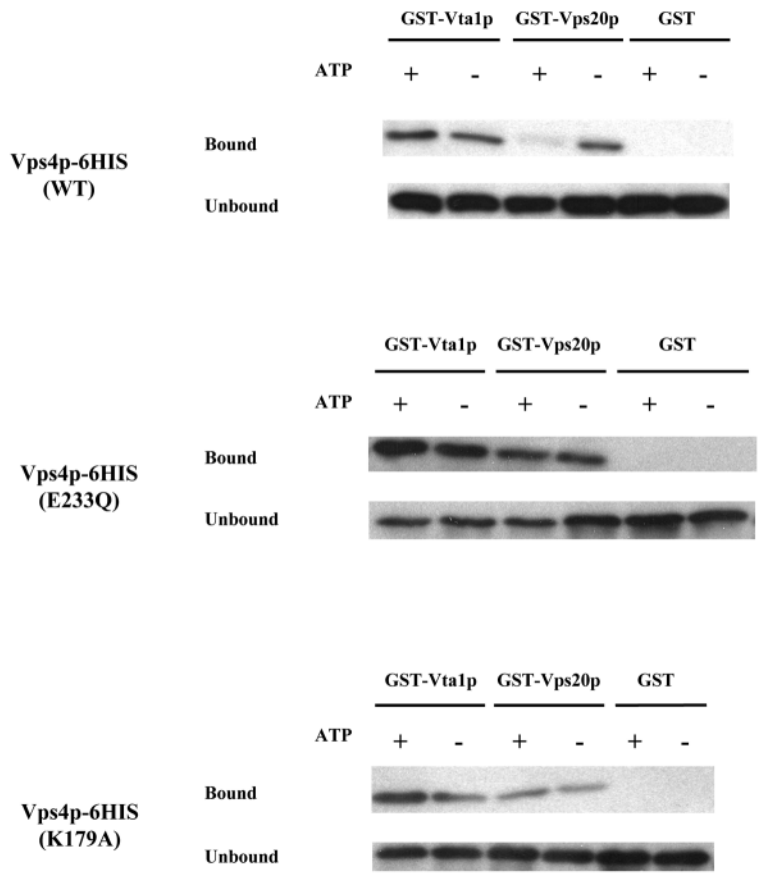

Fig. 3. Vps4p directly binds Vps20p and Vta1p in vitro and binding is ATP-independent. Wild-type Vps4p, and both ATP hydrolysis mutant (E233Q) and ATP binding mutant (K179A) forms of Vps4p were tagged at the C-terminus with 6HIS and expressed in *E. coli*. Each protein was affinity purified using the 6HIS tag and incubated with beads bearing GST-Vps20p, GST-Vta1p or GST only in the presence or absence of added ATP. Unbound proteins (unbound) were recovered in the supernatants. After washing the beads, the specifically bound proteins (bound) were eluted by heating in Laemmli sample buffer. Proteins in both bound and unbound samples were resolved by SDS-PAGE, and transferred to PVDF membranes. Wild-type and mutant forms of Vps4p-6HIS were detected by immunoblotting with a pentaHIS-specific monoclonal antiserum. In each set of experiments the exposure times for the gels containing bound and unbound samples were identical.

Discussion

Here, we report that *VPS20* and *VTA1* encode Vps4p-interacting proteins. Several lines of evidence support this conclusion. First, in a yeast two-hybrid screen with Vps4p as bait, we isolated multiple clones of *VPS20* and *VTA1*. Second, GST fusion constructs containing Vps20p or Vta1p associate with endogenous Vps4p in yeast lysates as well as bacterially expressed and purified Vps4p. Finally, deletion of *VPS20* or *VTA1* causes class E Vps$^-$ phenotypes similar to deletion of *VPS4* itself, suggesting that Vps20p and Vta1p function with Vps4p in vivo.

Vps20p and two other class E Vps proteins, Snf7p/Vps32p/Did1p (30% identity) and Mos10p/Vps60p/Chm5p (15% identity) comprise a gene family (Babst et al., 1998; Amerik et al., 2000; Kranz et al., 2001; Howard et al., 2001). Hspc177 (Genbank Acc. No. BC016698) encodes a mammalian protein with strong homology (21% identity) to yeast Vps20p over its full length. Other yeast family members include the class E Vps proteins Vps24p/Did3p, Did2p/Chm1p/Fti1p and Vps2p/Did4p/Ren1p/Chm2p (Davis et al., 1993; Babst et al., 1998; Amerik et al., 2000; Kranz et al., 2001; Howard et al., 2001). Proteins in this family all have extensive coiled-coil domains that can potentially mediate protein-protein interaction (Babst et al., 1998; Kranz et al., 2001; Howard et al., 2001); for example, in Vps20p the coiled-coil domain comprises residues 61-169 as predicted using the COILS algorithm (Lupas et al., 1991).

Although this is the first report of interaction between Vps4p and Vps20p, there have been two earlier reports of interactions between Vps4p and other family members: (1) a genomic two-hybrid screen identified an interaction between Vps4p and Snf7p/Vps32p (Uetz et al., 2000), and (2) a yeast two-hybrid screen using CHMP1 (the mammalian homologue of yeast Did2p/Chm1p) as bait led to the identification of human Vps4-A/SKD1 as a CHMP1 interactor (Howard et al., 2001). Interestingly, Did2p/Chm1p is among the other Vps4p two-hybrid interactors we identified in our screen (M. Wagle and A. Munn, unpublished).

Four of the six known coiled-coil class E Vps proteins (viz. Vps20p, Snf7p, Vps2p and Vps24p) have recently been shown to form a large protein complex known as ESCRTIII implicated in concentration and sorting of cargo proteins at the MVB prior to incorporation into intralumenal vesicles (Babst et al., 2002). In *vps4Δ* mutants, all four ESCRTIII proteins redistribute from the cytoplasm to the surface of endosomal membranes (Babst et al., 1998; Babst et al., 2002). Based on this in vivo data, it has been suggested that Vps4p uses the energy of ATP hydrolysis to break coiled-coil interactions and release ESCRTIII proteins from the surface of endosomes into the cytoplasm. ATP-dependent release of ESCRTIII proteins from endosomal membranes by Vps4p has yet to be demonstrated in vitro, however a mutant form of human Vps4-A (E228Q) that is locked in the ATP-bound state exhibits enhanced association with CHMP1 (Howard et al., 2001). This data supports the conclusion that in the ATP-bound form Vps4p associates with class E Vps proteins and breaks coiled-coil interactions.

We have shown here that binding of Vps4p to Vps20p in vitro is independent of ATP. A Vps4p ATP hydrolysis mutant (E233Q) exhibited increased binding to Vps20p in vitro compared with wild-type Vps4p, however an ATP binding mutant (K179A) also exhibited increased association (Fig. 3). Thus, enhanced binding to coiled-coil proteins may be a feature of non-functional (rather than ATP-bound) Vps4p. This is consistent with the observation that an ATP-binding mutant of mammalian Vps4-A (KQ) behaves like an ATP hydrolysis mutant (EQ) in exhibiting enhanced localisation to endosomes (Bishop and Woodman, 2000). ATP-independent association

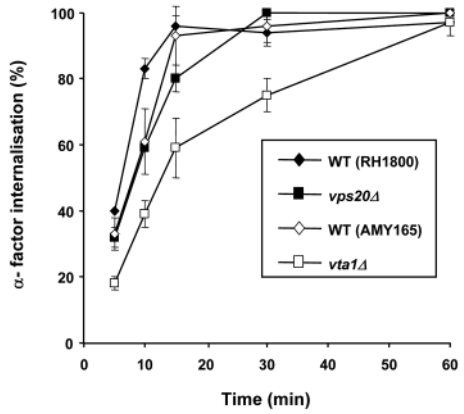

Fig. 4. Loss of Vps20p or Vta1p causes only slightly altered kinetics of α-factor internalisation. Wild-type (RH1800) and *vps20Δ* (AMY174), and wild-type (AMY165) and *vta1Δ* (AMY162) cells were grown to early exponential phase and assayed for [^{35}S]α-factor internalisation at 30°C. After addition of the [^{35}S]α-factor, samples were taken in duplicate at various time points and washed in either phosphate buffer pH 6 (removes unbound [^{35}S]α-factor) or citrate buffer pH 1 (removes bound but non-internalised [^{35}S]α-factor). Shown is the internalised α-factor as a percentage of the bound α-factor at each time point.

with coiled-coil domain proteins may distinguish Vps4p from other AAA-ATPases, such as NEM-sensitive fusion protein (NSF/Sec18p). NSF/Sec18p forms a 20S complex with soluble NSF attachment protein (α-SNAP) and α-SNAP-receptors (SNARES) and uses ATP hydrolysis to break coiled-coil interactions between SNARES. An NSF/Sec18p mutant protein with a mutation in the first of its two AAA-domains (D1) that prevents ATP binding is unable to associate with the α-SNAP-SNARE complex in vitro (Nagiec et al., 1995). Nevertheless, our analysis strongly supports the view that ATP hydrolysis by Vps4p dissociates coiled-coil interactions as proposed by Babst et al. (Babst et al., 1998; Babst et al., 2002). Interaction of Vps4p with Vps20p appears to involve coiled-coil interactions (Tables 3, 4) and is sensitive to ATP hydrolysis (Fig. 3).

ESCRTIII comprises Vps20p-Snf7p and Vps2p-Vps24p subcomplexes (Babst et al., 2002). The Vps2p-Vps24p subcomplex has been proposed to mediate recruitment of Vps4p to endosomes based on the finding that accumulation of ATP-locked Vps4p-E233Q mutant protein on endosomes is affected in *vps2* and *vps24* mutants (*vps20* and *snf7* mutants were not tested) (Babst et al., 2002). Our data suggest that Vps20p may also be important for recruitment of Vps4p to membranes. Vps20p is myristoylated and associates strongly with membranes (Ashrafi et al., 1998; Babst et al., 2002). Interestingly, myristoylation is not required for Vps20p interaction with Vps4p as Vps20p fusions lacking the myristoylation motif (MG, residues 1-2) still exhibit strong two-hybrid interaction with Vps4p. Furthermore, bacterially expressed Vps20p binds Vps4p in vitro and bacteria lack the ability to perform myristoylation. Our data show that Vps20p interacts with the N-terminal coiled-coil domain of Vps4p essential for Vps4p association with endosomal membranes (Babst et al., 1998). That Vps4p-E233Q and Vps4p-K179A mutant proteins exhibit increased association with Vps20p

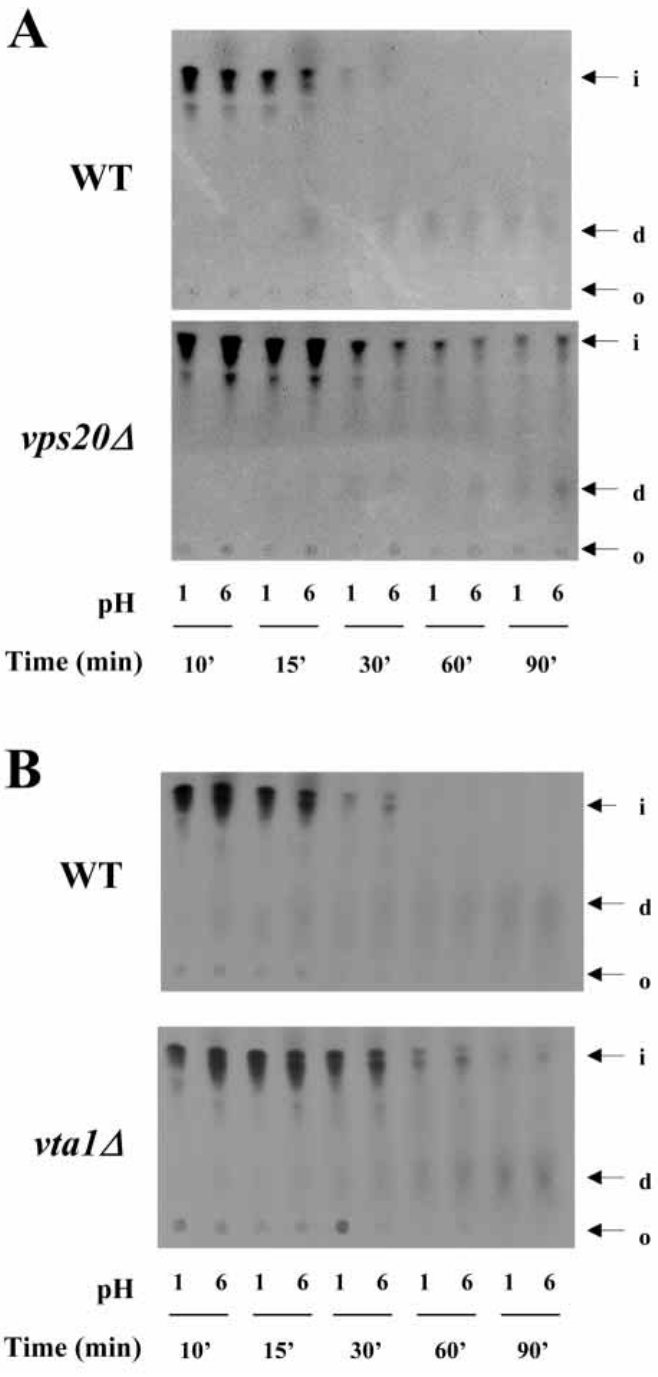

Fig. 5. Loss of Vps20p or Vta1p causes defects in α-factor degradation. Wild-type (RH1800) and *vps20Δ* (AMY174) (A), and wild-type (AMY165) and *vta1Δ* (AMY162) (B) cells were grown to early exponential phase and assayed for [^{35}S]α-factor transport to the vacuole and degradation at 30°C. [^{35}S]α-factor was prebound to the cells on ice and then the cells were harvested at 4°C and resuspended in fresh YPUAD and incubated at 30°C. At the time points shown, samples were taken in duplicate and washed in either phosphate buffer pH6 (removes unbound [^{35}S]α-factor) or citrate buffer pH 1 (removes bound non-internalised [^{35}S]α-factor). Lysates were prepared from each sample of cells and subjected to thin layer chromatography to separate intact (i) and degraded (d) [^{35}S]α-factor, which were visualised by fluorography at –80°C. 6, washed in pH 6 buffer; 1, washed in pH 1 buffer; o, origin where samples were loaded.

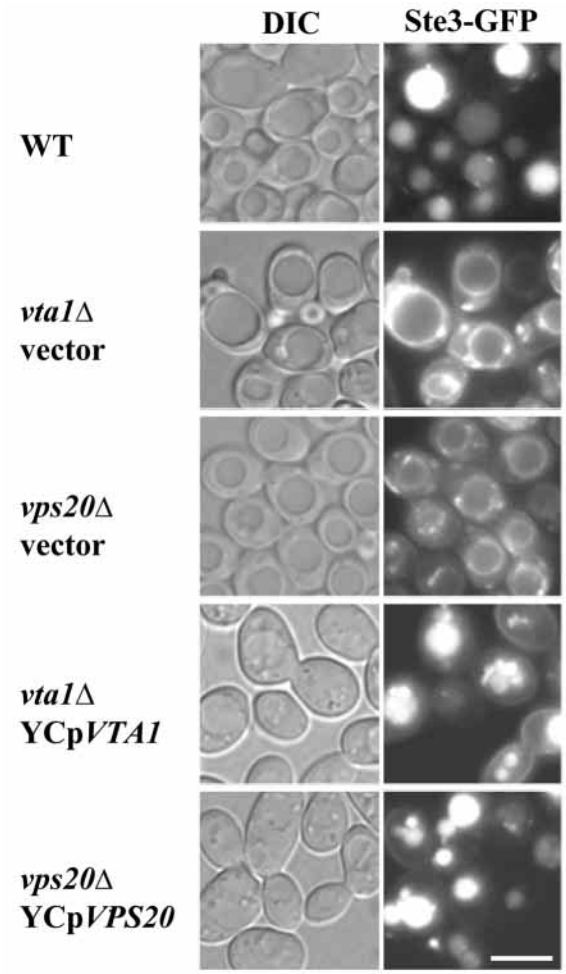

Fig. 6. Loss of Vps20p or Vta1p causes defects in Ste3p localisation to the vacuole. Wild-type (SF838-9D), *vps20* (SF838-9D*vpl10*) and *vta1* (PLY3046) cells were transformed with a low-copy plasmid encoding Ste3-GFP in combination with an empty *URA3* containing centromeric plasmid or centromeric plasmid containing the wild-type *VTA1* or *VPS20* gene as indicated. The localisation of Ste3-GFP was then assessed by fluorescence microscopy together with DIC imaging to identify yeast vacuoles. Cells were resuspended in 1% sodium azide, 1% sodium fluoride, 100 mM Tris pH 8.0 prior to fluorescence and DIC microscopy. Bar, 5 μm.

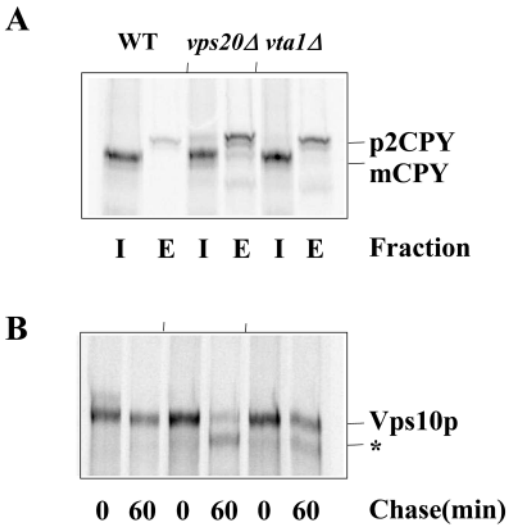

Fig. 7. Loss of Vps20p or Vta1p causes secretion of Golgi-modified p2 CPY precursor and degradation of Vps10p. Wild-type (SF838-9D), *vps20Δ* (SF838-9D*vpl10*) and *vta1Δ* (PLY3046) cells were converted to *PEP4* as described in Materials and Methods. They were pulse-labelled with [^{35}S]methionine/cysteine for 10 minutes at 30°C and then chased with excess unlabelled methionine/cysteine at the same temperature. Samples were taken at 0 or 60 minutes of chase, and further membrane transport was stopped by addition of sodium azide and sodium fluoride to 20 mM. The cells in each sample were converted to spheroplasts and fractionated into intracellular (I) and extracellular (E) fractions. CPY was immunoprecipitated from half the intracellular (I) and extracellular (E) fractions of the 60-minute chase samples (A). Vps10p was immunoprecipitated from the intracellular (I) fractions of the 0- and 60-minute chase samples (B). Indicated are the mature (mCPY) and Golgi-modified (p2CPY) forms of CPY, and both full-length Vps10p (Vps10p) and the lower protease-cleaved band of Vps10p (*).

correlates well with reports that both mutant proteins also exhibit increased accumulation on endosomes in vivo (Babst et al., 1998; Bishop and Woodman, 2000). The strength of Vps4p-Vps20p interaction may be an important determinant of Vps4p subcellular localization.

YLR181c (*VTA1*) is a novel class E *VPS* gene. Although Vta1p does not share significant homology to other class E Vps proteins, a putative mammalian homologue is encoded by dopamine-responsive gene (Drg-1) (GenBank Acc. No. AF271994) [also known as LYST-interacting protein 5 (Lip5) (GenBank Acc. No. AF141341)]. Drg-1/Lip5 has strong homology to Vta1p over N- (24% identity) and C-terminal (59% identity) sequences representing 43% of the total length of the protein. LYST is the protein affected in the human inherited immune and neurological disorder Chediak-Higashi Syndrome (CHS) and in *beige* mutant mice. Defects in endosomal membrane transport and lysosome morphology have been reported in CHS (Tchernev et al., 2002). The best yeast homologue of LYST is Bps1p, however deletion of *BPS1* in the SF838-9D background gave no class E *vps* phenotypes (R. C. Piper, unpublished).

Vta1p has two predicted coiled-coil domains (1stCC and 2ndCC comprising residues 35-63 and 232-263, respectively). The latter is encoded by all of our positive two-hybrid library clones, but our interaction domain analysis shows that Vps4p does not interact with the 1stCC or the 2ndCC domain of Vta1p. Instead, Vps4p interacts specifically with a short (65 residue) domain located at the extreme Vta1p C-terminus that lacks predicted coiled-coil structure. Furthermore, Vps4p binds to Vta1p via its acidic C-terminal domain (Tables 3, 4). Hence, coiled-coil interaction does not appear to mediate Vps4p interaction with Vta1p. This suggests that Vps4p may interact quite differently with Vta1p compared with coiled-coil Vps20p-family proteins. Vta1p may represent a stable subunit rather than a substrate of the Vps4p complex. Consistent with this, Vps4p binding to Vps20p in vitro is sensitive to ATP hydrolysis, whereas binding to Vta1p is unaffected by the presence or absence of ATP (Figs 2, 3). Little is known about the role of the C-terminal acidic domain in Vps4p function. In the case of another AAA-family ATPase, Hsp104p, the acidic C-terminal domain regulates ATP hydrolysis by the AAA

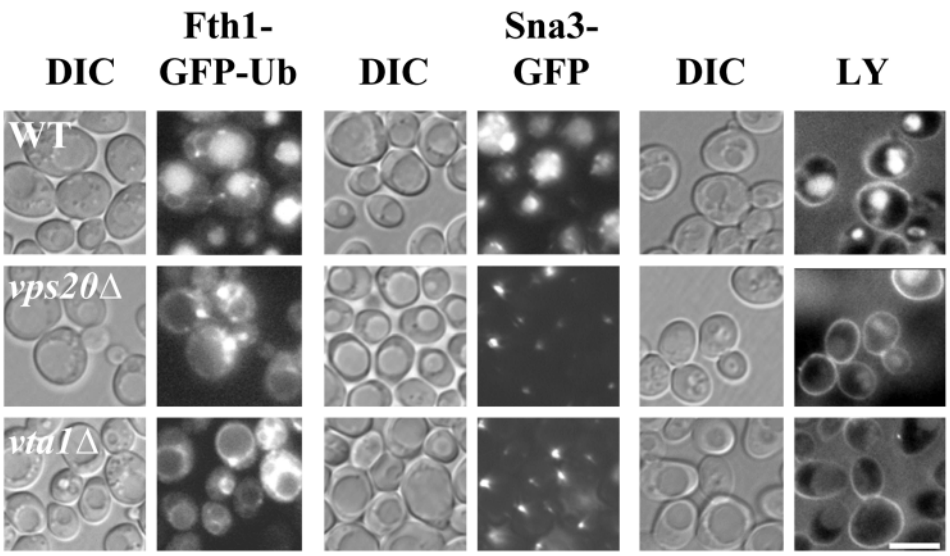

Fig. 8. Vps20p and Vta1p are required for multivesicular body sorting and LY accumulation in the vacuole. The two MVB reporter proteins, Fth1-GFP-Ub (left) and Sna3-GFP (centre) were localised in wild-type (SF838-9D), *vps20Δ* (SF838-9D*vpl10*) and *vta1Δ* (PLY3046) cells. For visualisation of Fth1-GFP-Ub, cells were grown in 100 μM of the iron chelator BPS for 6 hours prior to microscopy. Cells were resuspended in 1% sodium azide, 1% sodium fluoride, 100 mM Tris pH 8.0 prior to microscopy. Endocytosis of LY (right) was measured by incubating cells in media containing LY for 60 minutes at 30°C, washing and viewing the cells by DIC and fluorescence microscopy. Bar, 5 μm.

domain (Cashikar et al., 2002). Although this is not known for Vps4p, it is intriguing to speculate that Vta1p regulates the ATPase activity of Vps4p.

Loss of Vps20p or Vta1p confers classical class E Vps$^-$ phenotypes similar to loss of Vps4p, including: 1) a block in MVB sorting of endocytosed surface proteins, vacuolar membrane proteins and the lipid NBD-PC; 2) accumulation of endocytosed surface proteins (e.g. Ste3p), lipid-soluble endocytic dyes (e.g. FM4-64) and vacuolar membrane proteins (e.g. CPS, Sna3p) in the 'class E' compartment; and 3) secretion of Golgi-modified p2CPY. As in other class E *vps* mutants, p2CPY secretion is associated with degradation of Vps10p. In wild-type cells Vps10p is stable and cycles from the late Golgi to the PVC during the sorting of soluble vacuolar hydrolases to the PVC. In class E *vps* mutants Vps10p and vacuolar hydrolases are trapped in the class E compartment and Vps10p is degraded. Some phenotypic characterisation has already been reported for *vps20*, but this is the first report that *vta1* mutants have class E *vps* phenotypes.

Our results suggest that vacuolar delivery of Sna3p may have unique requirements. Although Ste3-GFP, Fth1-GFP-Ub (Figs 6, 8) and GFP-Cps1p (data not shown) localise to both the class E compartment and the vacuole limiting membrane in class E *vps* mutants, Sna3-GFP appears to exclusively localise to the class E compartment (Fig. 8). Unlike the ubiquitin-dependent MVB sorting of other proteins (Urbanowski and Piper, 2001; Katzmann et al., 2001), MVB sorting of Sna3p is ubiquitin-independent. It has been proposed that MVB sorting of

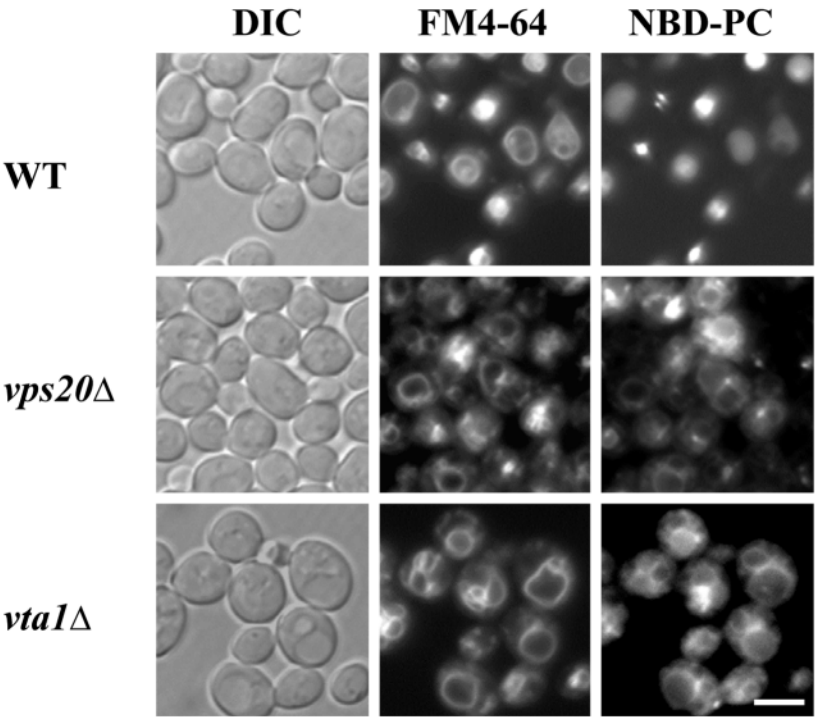

Fig. 9. Vps20p and Vta1p are required for MVB lipid sorting. Sorting of the lipid dye NBD-PC was followed in wild-type (SF838-9D), *vps20Δ* (SF838-9D*vpl10*) and *vta1Δ* (PLY3046) cells. Cells labelled at 30°C with FM4-64 (2 μM) in potassium phosphate-buffered YPUAD (pH 7.0) for 20 minutes followed by incubation with NBD-PC (100 μM) for an additional 20 minutes. Cells were washed and resuspended in SD media and incubated for an additional 30 minutes at 30°C prior to fluorescence microscopy. Cells were resuspended in 1% sodium azide, 1% sodium fluoride, 100 mM Tris pH 8.0 prior to fluorescence and DIC microscopy. Bar, 5 μm.

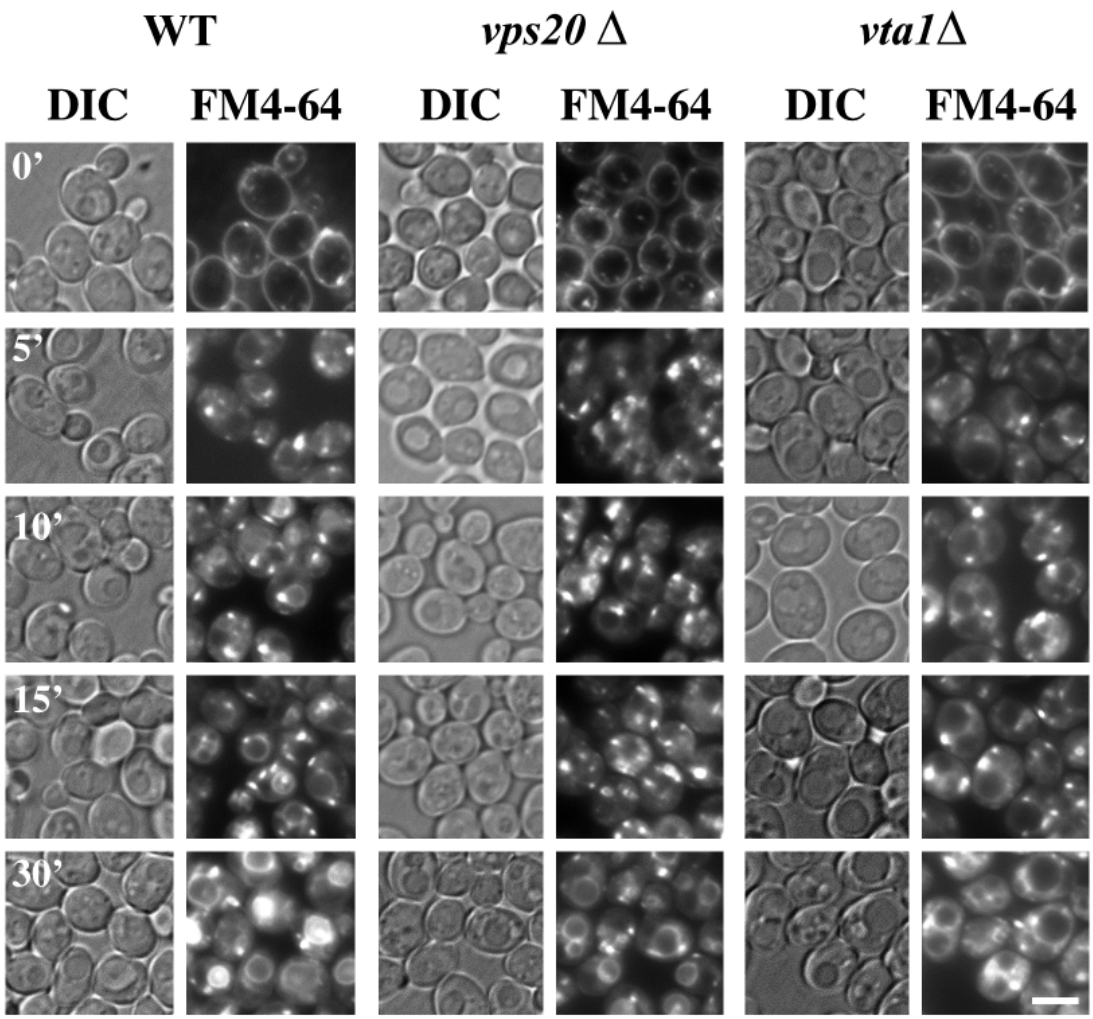

Fig. 10. Vps20p and Vta1p are required for transport of FM4-64 from late endosomes to the vacuole. Wild-type (SF838-9D), *vps20Δ* (SF838-9D*vpl10*) and *vta1Δ* (PLY3046) cells were grown to early exponential phase and then incubated with 2 μM FM4-64 at 0°C for 30 minutes. Cells were washed in ice-cold YPUAD and resuspended in YPUAD at 30°C without FM4-64 (0'). Cell aliquots were removed at the indicated times after shift to 30°C (5', 10', etc.), washed in 1% sodium azide, 1% sodium fluoride, 100 mM Tris pH 8.0, and viewed by fluorescence and DIC microscopy. Bar, 5 μm.

Sna3p occurs via spontaneous partitioning of the Sna3p transmembrane domains into subdomains of the MVB limiting membrane that form intralumenal vesicles (Reggiori and Pelham, 2001). The unique properties of the Sna3p transmembrane domains may thus prevent Sna3p from entering endosome to vacuole transport intermediates, leading to Sna3p retention in endosomes. Alternatively, Sna3p, but not CPS, Ste3p or Fth1-Ub, could possess the ability to recycle from the vacuole to the MVB in wild-type cells. If exit from the vacuole is relatively unaffected compared with exit from the class E compartment in class E *vps* mutants, Sna3p would redistribute from the vacuole to the class E compartment. Ultimately, an understanding of these sorting differences requires insight into the biological function of Sna3p, however a function for Sna3p has not yet been ascribed.

We thank J. Wang for critical reading of the manuscript, S. Vasudevan, B. Winsor, A. Wach, P. Philippsen, U. Surana, M. Cai, T. Stevens, M. Babst, D. Katzmann and S. Emr for strains and constructs, and R. Tsien (HHMI, UCSD, La Jolla, CA, USA) for permission to use the S65T mutant GFP. We thank the IMA/TLL DNA sequencing facility. This work was made possible by funding from A*STAR (Singapore) and National Health and Medical Research Council of Australia Project Grant 252750 to A.L.M., from the National Medical Research Council of Singapore to H.Y., and by NIH RO1 GM58202 to R.C.P.

References

Adams, A., Gottschling, D. E., Kaiser, C. A. and Stearns, T. (1997). *Methods in Yeast Genetics. A Cold Spring Harbor Laboratory Course Manual*. Cold Spring Harbor, NY, USA: Cold Spring Harbor Laboratory Press.

Amerik, A. Y., Nowak, J., Swaminathan, S. and Hochstrasser, M. (2000). The Doa4 deubiquitinating enzyme is functionally linked to the vacuolar protein-sorting and endocytic pathways. *Mol. Biol. Cell* **11**, 3365-3380.

Ashrafi, K., Farazi, T. A. and Gordon, J. I. (1998). A role for *Saccharomyces cerevisiae* fatty acid activation protein 4 in regulating protein N-myristoylation during entry into stationary phase. *J. Biol. Chem.* **273**, 25864-25874.

Babst, M., Sato, T. K., Banta, L. M. and Emr, S. D. (1997). Endosomal transport function in yeast requires a novel AAA-type ATPase, Vps4p. *EMBO J.* **16**, 1820-1831.

Babst, M., Wendland, B., Estepa, E. J. and Emr, S. D. (1998). The Vps4p AAA ATPase regulates membrane association of a Vps protein complex required for normal endosome function. *EMBO J.* **17**, 2982-2993.

Babst, M., Katzmann, D. J., Estepa-Sabal, E. J., Meerloo, T. and Emr, S. D. (2002). ESCRT-III: an endosome-associated heterooligomeric protein complex required for MVB sorting. *Dev. Cell* **3**, 271-282.

Bilodeau, P. S., Urbanowski, J. L., Winistorfer, S. C. and Piper, R. C. (2002). The Vps27p-Hse1p complex binds ubiquitin and mediates endosomal protein sorting. *Nat. Cell Biol.* **4**, 534-539.

Bishop, N. and Woodman, P. (2000). ATPase-defective mammalian *VPS4* localizes to aberrant endosomes and impairs cholesterol trafficking. *Mol. Biol. Cell* **11**, 227-239.

Bryant, N. J. and Stevens, T. H. (1998). Vacuole biogenesis in *Saccharomyces cerevisiae*, protein transport pathways to the yeast vacuole. *Microbiol. Mol. Biol. Rev.* **62**, 230-247.

Cashikar, A. G., Schirmer, E. C., Hattendorf, D. A., Glover, J. R., Ramakrishnan, M. S., Ware, D. M. and Lindquist, S. L. (2002). Defining a pathway of communication from the C-terminal peptide binding domain to the N-terminal ATPase domain in a AAA protein. *Mol. Cell* **9**, 751-760.

Cereghino, J. L., Marcusson, E. G. and Emr, S. D. (1995). The cytoplasmic tail domain of the vacuolar protein sorting receptor Vps10p and a subset of *VPS* gene products regulate receptor stability, function, and localization. *Mol. Biol. Cell* **6**, 1089-1102.

Davis, N. G., Horecka, J. L. and Sprague, G. F., Jr (1993). Cis- and trans-acting functions required for endocytosis of the yeast pheromone receptors. *J. Cell Biol.* **122**, 53-65.

Dower, W. J., Miller, J. F. and Ragsdale, C. W. (1988). High efficiency transformation of *E. coli* by high voltage electroporation. *Nucleic Acids Res.* **16**, 6127-6145.

Dulic, V., Egerton, M., Elguindi, I., Raths, S., Singer, B. and Riezman, H. (1991). Yeast endocytosis assays. *Methods Enzymol.* **194**, 697-710.

Finken-Eigen, M., Rohricht, R. A. and Kohrer, K. (1997). The *VPS4* gene is involved in protein transport out of a yeast pre-vacuolar endosome-like compartment. *Curr. Genet.* **31**, 469-480.

Forsberg, H., Hammar, M., Andreasson, C., Moliner, A. and Ljungdahl, P. O. (2001). Suppressors of *ssy1* and *ptr3* null mutations define novel amino acid sensor-independent genes in *Saccharomyces cerevisiae*. *Genetics* **158**, 973-988.

Gietz, R. D. and Sugino, A. (1988). New yeast-*Escherichia coli* shuttle vectors constructed with in vitro mutagenized yeast genes lacking six-base pair restriction sites. *Gene* **74**, 527-534.

Gyuris, J., Golemis, E., Chertkov, H. and Brent, R. (1993). Cdi1, a human G1 and S phase protein phosphatase that associates with Cdk2. *Cell* **75**, 791-803.

Hanson, P. K., Grant, A. M. and Nichols, J. W. (2002). NBD-labeled phosphatidylcholine enters the yeast vacuole via the pre-vacuolar compartment. *J. Cell Sci.* **115**, 2725-2733.

Hicke, L., Zanolari, B., Pypaert, M., Rohrer, J. and Riezman, H. (1997). Transport through the yeast endocytic pathway occurs through morphologically distinct compartments and requires an active secretory pathway and Sec18p/N-ethylmaleimide-sensitive fusion protein. *Mol. Biol. Cell* **8**, 13-31.

Howard, T. L., Stauffer, D. R., Degnin, C. R. and Hollenberg, S. M. (2001). CHMP1 functions as a member of a newly defined family of vesicle trafficking proteins. *J. Cell Sci.* **114**, 2395-2404.

Katzmann, D. J., Babst, M. and Emr, S. D. (2001). Ubiquitin-dependent sorting into the multivesicular body pathway requires the function of a conserved endosomal protein sorting complex, ESCRT-1. *Cell* **106**, 145-155.

Katzmann, D. J., Odorizzi, G. and Emr, S. D. (2002). Receptor downregulation and multivesicular-body sorting. *Nat. Rev.* **3**, 893-905.

Kranz, A., Kinner, A. and Kolling, R. (2001). A family of small coiled-coil-forming proteins functioning at the late endosome in yeast. *Mol. Biol. Cell* **12**, 711-723.

Kübler, E. and Riezman, H. (1993). Actin and fimbrin are required for the internalisation step of endocytosis in yeast. *EMBO J.* **12**, 2855-2862.

Longtine, M. S., McKenzie, A., DeMarini, D. J., Shah, N. G., Wach, A., Brachat, A., Philippsen, P. and Pringle, J. R. (1998). Additional modules for versatile and economical PCR-based gene deletion and modification in *Saccharomyces cerevisiae*. *Yeast* **14**, 953-961.

Lupas, A., Van Dyke, M. and Stock, J. (1991). Predicting coiled coils from protein sequences. *Science* **252**, 1162-1164.

Mellman, I. (1996). Endocytosis and molecular sorting. *Annu. Rev. Cell Dev. Biol.* **12**, 575-625.

Mulholland, J., Konopka, J., Singer-Krüger, B., Zerial, M. and Botstein, D. (1999). Visualization of receptor-mediated endocytosis in yeast. *Mol. Biol. Cell* **10**, 799-817.

Munn, A. L. and Riezman, H. (1994). Endocytosis is required for the growth of vacuolar H^+-ATPase-defective yeast, identification of six new *END* genes. *J. Cell Biol.* **127**, 373-386.

Munn, A. L., Stevenson, B. J., Geli, M. I. and Riezman, H. (1995). *end5*, *end6*, and *end7*, mutations that cause actin delocalization and block the internalization step of endocytosis in *Saccharomyces cerevisiae*. *Mol. Biol. Cell* **6**, 1721-1742.

Munn, A. L., Heese-Peck, A., Stevenson, B. J., Pichler, H. and Riezman, H. (1999). Specific sterols required for the internalization step of endocytosis in yeast. *Mol. Biol. Cell* **10**, 3943-3957.

Munn, A. L. (2000). The yeast endocytic membrane transport system. *Microsc. Res. Tech.* **51**, 547-562.

Nagiec, E. E., Bernstein, A. and Whiteheart, S. W. (1995). Each domain of the N-ethylmaleimide-sensitive fusion protein contributes to its transport activity. *J. Biol. Chem.* **270**, 29182-29188.

Odorizzi, G., Babst, M. and Emr, S. D. (1998). Fab1p PtdIns(3)P 5-kinase function essential for protein sorting in the multivesicular body. *Cell* **95**, 847-858.

Piper, R. C., Cooper, A. A., Yang, H. and Stevens, T. H. (1995). *VPS27* controls vacuolar and endocytic traffic through a prevacuolar compartment in *Saccharomyces cerevisiae*. *J. Cell Biol.* **131**, 603-617.

Piper, R. C. and Luzio, J. P. (2001). Late endosomes: sorting and partitioning in multivesicular bodies. *Traffic* **2**, 612-621.

Prescianotto-Baschong, C. and Riezman, H. (1998). Morphology of the yeast endocytic pathway. *Mol. Biol. Cell* **9**, 173-189.

Prescianotto-Baschong, C. and Riezman, H. (2002). Ordering of compartments in the yeast endocytic pathway. *Traffic* **3**, 37-49.

Raymond, C. K., Howald-Stevenson, I., Vater, C. A. and Stevens, T. H. (1992). Morphological classification of the yeast vacuolar protein sorting mutants, evidence for a prevacuolar compartment in class E *vps* mutants. *Mol. Biol. Cell* **3**, 1389-1402.

Reggiori, F. and Pelham, H. R. (2001). Sorting of proteins into multivesicular bodies: ubiquitin-dependent and -independent targeting. *EMBO J.* **20**, 5176-5186.

Rieder, S. E., Banta, L. M., Kohrer, K., McCaffery, J. M. and Emr, S. D. (1996). Multilamellar endosome-like compartment accumulates in the yeast *vps28* vacuolar protein sorting mutant. *Mol. Biol. Cell* **7**, 985-999.

Tchernev, V. T., Mansfield, T. A., Giot, L., Kumar, A. M., Nandabalan, K., Li, Y., Mishra, V. S., Detter, J. C., Rothberg, J. M. and Wallace, M. R. et al. (2002). The Chediak-Higashi protein interacts with SNARE complex and signal transduction proteins. *Mol. Med.* **8**, 56-64.

Uetz, P., Giot, L., Cagney, G., Mansfield, T. A., Judson, R. S., Knight, J. R., Lockshon, D., Narayan, V., Srinivasan, M. and Pochart, P. et al. (2000). A comprehensive analysis of protein-protein interactions in *Saccharomyces cerevisiae*. *Nature* **403**, 623-627.

Urbanowski, J. L. and Piper, R. C. (2001). Ubiquitin sorts proteins into the intralumenal degradative compartment of the late-endosome/vacuole. *Traffic* **2**, 622-630.

Vida, T. A. and Emr, S. D. (1995). A new vital stain for visualizing vacuolar membrane dynamics and endocytosis in yeast. *J. Cell Biol.* **128**, 779-792.

Zahn, R., Stevenson, B. J., Schröder-Köhne, S., Zanolari, B., Riezman, H. and Munn, A. L. (2001). End13p/Vps4p is required for efficient transport from early to late endosomes in *Saccharomyces cerevisiae*. *J. Cell Sci.* **114**, 1935-1947.